Inhibition of salt-inducible kinases 2 and 3 reduces inflammatory signature in psoriasis

JIDOpen

Anna Caroline Pilz[1,2,3], Eva Briem[4,5], Maikel Colli[6], Christina Hillig[5], Stephanie Lavazais[7], Michael P. Menden[5,8], Tilo Biedermann[2], Felix Lauffer[2,9], Kilian Eyerich[1,2,10], Steve De Vos[6,11] and Manja Jargosch[2,3,11]

Journal of Investigative Dermatology (2026) ■, ■–■; doi:10.1016/j.jid.2026.07.033

Psoriasis is a highly prevalent inflammatory skin disease for which good systemic therapeutic agents are available. However, there is still a great need for new treatment options, especially oral ones. Salt-inducible kinases (SIKs) are emerging as new druggable targets in immune diseases, and the SIK2/SIK3 inhibitor GLPG3970 recently proved to efficiently reduce psoriasis lesions in a phase Ib trial. This study assesses the molecular events underlying the beneficial effects of SIK2/SIK3 inhibition through GLPG3970 in psoriasis. Using spatial transcriptomics and single-cell sequencing, abundant expression of *SIK2* and *SIK3* but not of *SIK1* was observed in psoriatic skin. In vitro, GLPG3970 reduced psoriasis marker cytokines and chemokines (TNF, IFNγ, IL-1β, IL-6, CXCL8, CXCL10) in peripheral mononuclear cells, T cells, and fibroblasts but not in keratinocytes. Bulk RNA sequencing of lesional psoriasis biopsies treated ex vivo with GLPG3970 and of biopsies received from responders versus placebo-treated patients from the clinical trial showed downregulation of inflammatory pathways with suppression of *IL1B*, *CXCL1*, *CXCL8*, *CEBPB*, *CD177*, and *CLEC5A* in both settings. In summary, this study suggests that specific inhibition of SIK2/SIK3 reduces acute-phase immunity and neutrophil recruitment in psoriasis.

Keywords: Acute inflammation, Dendritic cells, Macrophages, Monocytes, Neutrophils

INTRODUCTION

Psoriasis is a chronic inflammatory skin disease that clinically presents most frequently with erythematosquamous plaques. It affects between 0.05 and 6.60% of the adult population worldwide, with the highest prevalence rates in Australasia, western/central Europe, North America, and high-income Latin America (Parisi et al, 2020). About 20% of people with psoriasis display moderate-to-severe involvement, potentially qualifying them for systemic treatment (Armstrong et al, 2021). Here, more than 10 therapies targeting different structures are currently approved (Sieminska et al, 2024). The most effective therapies belong to the group of biologics—antibodies that specifically block 1 or 2 cytokines or a receptor that is part of the T helper (Th) 17 or TNF pathway (Sbidian et al, 2022). Nevertheless, in real-world analyses, only 46.2% of patients achieve a PASI75 after 1 year of treatment with a biologic (Van Muijen et al, 2022). In addition, biologics, as large protein complexes, need to be stored refrigerated and injected. Hence, oral treatment options are desirable. Today, 2 modern, moderately potent tablets are on the market, namely, apremilast and deucravacitinib. However, in a phase III study, they only reached PASI75 of 35.1% and 58.4%, respectively, at week 16 (Armstrong et al, 2023). Consequently, there is still a high need for new, especially orally administered, treatments.

Salt-inducible kinases (SIKs) are a subfamily of 3 isoforms (SIK1, SIK2, and SIK3) that belong to the family of adenosine monophosphate-activated protein kinases and have recently emerged as new druggable targets in immune diseases, such as inflammatory bowel disease (Babbe et al, 2024). Here, SIK2 and SIK3 seem to be of greater importance than SIK1 in immune cell development and function regarding macrophages (Macs), T cells, and mast cells (Peixoto et al, 2024). GLPG3970, a selective direct SIK2/SIK3 inhibitor developed by Galapagos, leads to the downregulation of proinflammatory cytokines, such as TNF, and the upregulation of immunoregulatory mediators, such as IL-10, in human myeloid and lymphoid cell culture models. Furthermore, GLPG3970 is beneficial in murine colitis, arthritis, and psoriasis models (De Vos et al, 2026; Peixoto et al, 2024). In

[1]*Department of Dermatology and Venereology, Medical Center, University of Freiburg, Freiburg, Germany;* [2]*Department of Dermatology and Allergy, School of Medicine and Health, Technical University of Munich, Munich, Germany;* [3]*Center of Allergy and Environment (ZAUM), Technical University and Helmholtz Center Munich, Munich, Germany;* [4]*Anthropology and Human Genomics, Faculty of Biology, Ludwig-Maximilians-Universität München, Planegg-Martinsried, Germany;* [5]*Computational Health Center, Institute of Computational Biology, Helmholtz Munich, Munich, Germany;* [6]*Galapagos NV, Mechelen, Belgium;* [7]*Galapagos SASU, Romainville, France;* [8]*Department of Biochemistry and Pharmacology, Bio21 Molecular Science and Biotechnology Institute, The University of Melbourne, Parkville, Australia;* [9]*Department of Dermatology, Ludwig-Maximilians University Hospital, Munich, Germany; and* [10]*Division of Dermatology and Venereology, Department of Medicine Solna, Karolinska Institutet, Stockholm, Sweden*

[11]*These authors contributed equally to this work.*

Correspondence: Anna Caroline Pilz, Department of Dermatology and Venereology, Medical Center, University of Freiburg, Hauptstraße 7, Freiburg 79104, Germany. E-mail: anna.caroline.pilz@uniklinik-freiburg.de

Abbreviations: DC, dendritic cell; FC, fold change; LPS, lipopolysaccharide; Mac, macrophage; MO, monocyte; SIK, salt-inducible kinase; Th, T helper

Received 14 January 2026; revised 2 July 2026; accepted 2 July 2026; accepted manuscript published online XXX; corrected proof published online XXX.

© 2026 The Author(s). Published by Elsevier Inc. on behalf of Society for Investigative Dermatology. This is an open access article under the CC BY license (http://creativecommons.org/licenses/by/4.0/).

line with this, GLPG3970 showed promising results in a randomized, double-blind, placebo-controlled phase Ib study with 26 patients with psoriasis. A least squares mean PASI reduction of 36.6% ± 6.4 was seen after 6 weeks of treatment with 350 mg once daily (De Vos et al, 2026).

This study investigates direct target cells as well as the main immunological mechanisms underlying the potential efficacy of SIK2/SIK3 inhibition in the context of psoriatic disease.

RESULTS

SIK2 and SIK3 are abundantly expressed in psoriatic skin

To determine the extent to which *SIK1*, *SIK2*, and *SIK3* are expressed in psoriatic skin lesions, spatial transcriptomics was performed on skin biopsies from 9 patients with psoriasis. Whereas transcripts of *SIK1* were almost undetectable in lesional and/or nonlesional skin, *SIK2* and *SIK3* transcripts were abundantly expressed in lesional skin and upregulated compared with those in nonlesional skin (Figure 1a). Both *SIK2* and *SIK3* were mostly enriched in the basal epidermis and dermis depth 1, with *SIK3* being more strongly expressed than *SIK2* (Figure 1b). In addition, single-cell sequencing of lesional skin from 7 patients with psoriasis was performed (Figure 1c). *SIK2* was most strongly expressed by fibroblasts, vascular endothelial cells, and monocytes (MOs)/Macs/dendritic cells (DCs). *SIK3* was also abundantly expressed in these clusters and additionally in T cells, keratinocytes, and pericytes.

GLPG3970 treatment reduces inflammation in primary human PBMCs as well as in lesional T cells and fibroblasts from patients with psoriasis

Because SIK2 and SIK3, as opposed to SIK1, are abundant in lesional skin of patients with psoriasis and are expressed by various cell types, the effects of SIK2/SIK3 inhibition through GLPG3970 were examined in vitro in the major immune-relevant cell populations, namely, MOs/Macs/DCs, T cells, and keratinocytes. In addition, fibroblasts, recently increasingly identified as important players in psoriasis pathogenesis, were investigated. A comparison with the phosphodiesterase 4 inhibitor apremilast, as an approved psoriasis therapeutic agent with a partially overlapping mode of action, was performed.

First, SIK2/SIK3 was inhibited in lipopolysaccharide (LPS)-stimulated PBMCs from 6 patients with psoriasis in a whole blood assay. LPS stimulation strongly induced the production of numerous psoriasis-associated proteins, which in turn was reduced by the inhibition of SIK2/SIK3 by GLPG3970 (Figure 2a; Welch's t-test). Classical MO/Mac/DC-derived cytokines, such as IL-1β (69%, $P = .0012$), IL-6 (66%, $P = .0062$), and TNF (37%, $P = .0014$), as well as key T-cell cytokines, such as IFN-γ (72%, $P = .0098$), IL-17A (81%, $P = .0003$), and IL-2 (61%, $P = .0025$), were downregulated by GLPG3970 in LPS-stimulated cells. In addition, CXCL10 (60%, $P = .0009$), CCL2 (78%, $P = .0025$), and MIP-1β (66%, $P = .0003$) were decreased by GLPG3970. In comparison to GLPG3970, apremilast only led to the suppression of TNF (78%, $P = .0414$) and CXCL10 (86%, $P \leq .0257$). Notably, IL-10 showed a trend toward induction with GLPG3970 and apremilast.

SIK2/SIK3 inhibition was then analyzed in lesional T cells isolated from skin biopsies of 4 patients with psoriasis. Cytokine production by αCD3/αCD28-activated lesional T cells was neutralized by GLPG3970 in the case of IL-22 (75%, $P = .0030$), TNF (85%, $P < .0001$), IFN-γ (83%, $P = .0059$), and also IL-10 (95%, $P < .0001$) (Figure 2b; Welch's t-test). IL-17A was not regulated by SIK2/SIK3 inhibition, but IL-17A levels were also close to the detection limit. Finally, GLPG3970- and apremilast-mediated effects were investigated in IL-1β– and IL-17A–stimulated keratinocytes and in IL-1β–stimulated fibroblasts. In keratinocytes, no regulation of psoriasis-related genes such as *DEFB4A*, *CXCL8*, *IL6*, *LCE3A*, and *TNF* by GLPG3970 was observed (Supplementary Figure S1; Welch's t-test). However, in fibroblasts, downregulation of *CXCL5* (52%, $P = .0240$), *CXCL8* (45%, $P = .0152$), and *TNF* (65%, $P = .0163$) by GLPG3970 was seen compared with that in IL-1β–stimulated cells (Figure 2c; Welch's t-test). *CXCL8* (32%, $P = .0051$) and *TNF* (59%, $P = .0266$) were also significantly suppressed by apremilast. As in PBMCs, *IL-10* was not suppressed in fibroblasts.

Blocking SIK2/SIK3 ex vivo by GLPG3970 treatment reduced inflammation in psoriatic skin lesions

Having observed an efficient reduction of genes associated with psoriasis in vitro, in the next step, SIK2/SIK3 inhibition was investigated in cultured punch biopsies of lesional skin from patients with psoriasis (n = 5). After 24 hours of ex vivo treatment with GLPG3970, total RNA from the biopsies was isolated and analyzed by bulk RNA sequencing. Principal component analysis of all samples (Figure 3a) and hierarchical clustering of expression z-scores (Figure 3b) showed a clear separation between GLPG3970- and vehicle-treated control samples. Gene set enrichment analysis of the hallmark collection was performed to gain a general understanding of the regulated processes. Among the 26 suppressed pathways, "inflammatory response" as well as TNF, IL-6, IL-2, and TGF-β signaling and "IFN-γ response" (all adjusted $P < .0001$) were identified (Figure 3c). DESeq2 analysis revealed a total of 874 genes with statistically significant expression changes (adjusted $P < .05$) in GLPG3970-treated samples compared with that in vehicle controls. Of these, 189 genes were differentially expressed with an absolute $\log_2$ fold change (FC) > 1, comprising 175 downregulated and 14 upregulated genes (Figure 3d). The top downregulated genes were *K33B*, *CXCL5*, *PRR9*, *ZP4*, and *IL24* ($\log_2$FC = −4.4, −3.9, −3.3, −3.1, and −2.7, respectively). Regarding psoriasis-associated chemokines and cytokines, *CXCL1*, *CXCL5*, and *CXCL8* ($\log_2$FC = −1.3, −3.9, and −1.8, respectively) as well as *IL1B*, *IL1A*, and *IL6* ($\log_2$FC = −1.8, −1.2, and −1.1, respectively) were significantly downregulated by GLPG3970, whereas Th17-associated genes such as *IL17A*, *IL17F*, *IL19*, *IL22*, *IL23A*, as well as *TNF* and *IFNG* were not regulated (Figure 3e). *CCL2* and *CCL4* along with the receptors *CCR1* and *CCR5* ($\log_2$FC = −1.0, −1.2, −1.1, and −1.1, respectively) were suppressed. Expression levels of genes indicating aberrant keratinization such as the marker keratins *K6*, *K16*, and *K17* and/or antimicrobial peptides such as the S100 proteins or *DEFB4A* and *DEFB4B* remained largely unchanged. However, *IVL*, *TGM2*, *LCE3C*, *SPRR1A*, and *SPRR3* ($\log_2$FC = −0.8, −1.2, −0.8, −0.9, and −2.7, respectively)

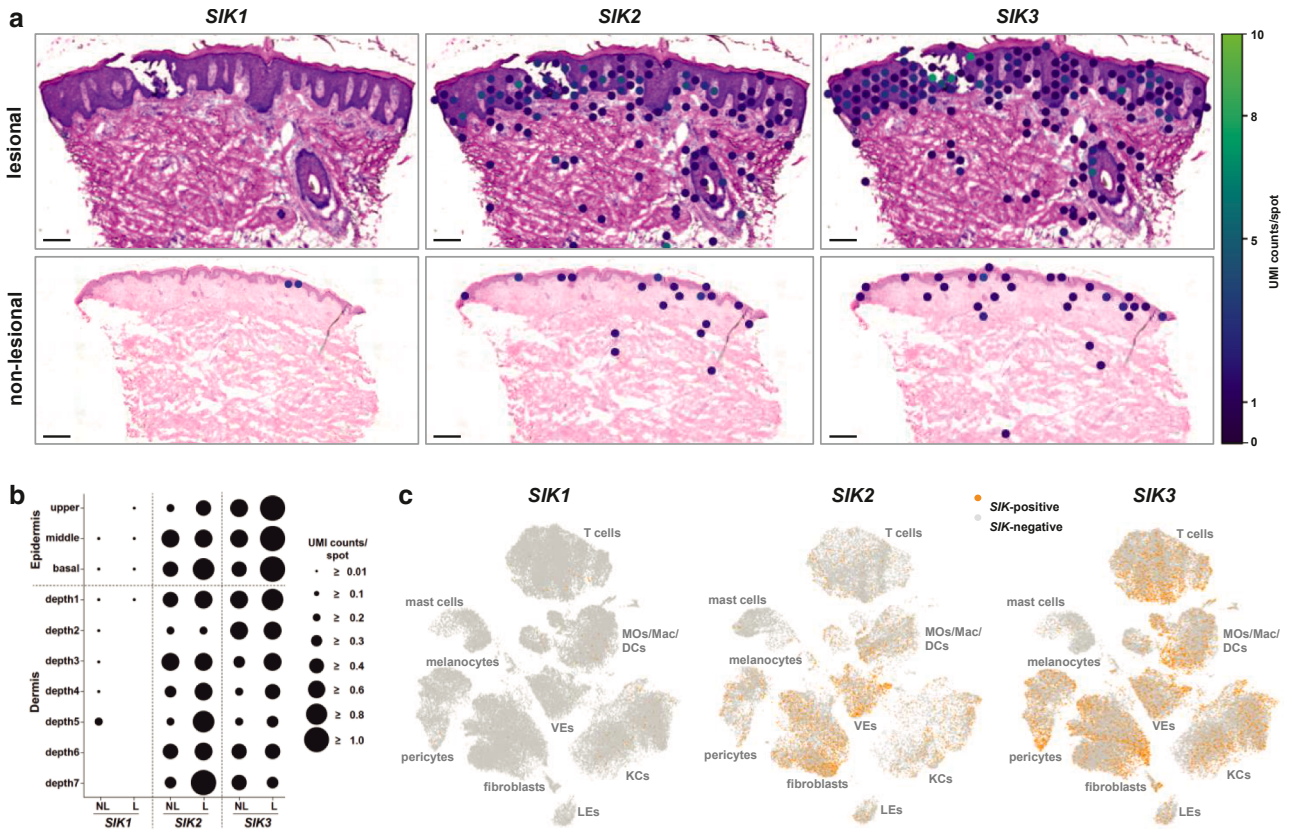


Figure 1. *SIK2* and *SIK3* are abundantly expressed in psoriatic skin. (**a, b**) Spatial expression of *SIK1*, *SIK2*, and *SIK3* in lesional ($n_{patients} = 9$) and nonlesional ($n_{patients} = 3$) psoriatic skin analyzed by spatial transcriptomics. (**a**) UMI counts per spot in H&E staining of a representative patient are shown (bar = 250 μm) and (**b**) quantified in the entire cohort, classified by upper, middle, and basal epidermis as well as 7 different dermis depths. (**c**) Cell type–specific expression of *SIK1*, *SIK2*, and *SIK3* from single-cell RNA-sequencing analysis of lesional psoriasis skin ($n_{patients} = 7$) visualized using UMAP plot. Orange denotes SIK-expressing cells. DC, dendritic cell; KC, keratinocyte; LE, lymphatic endothelial cell; Mac, macrophage; MO, monocyte; SIK, salt-inducible kinase; UMAP, Uniform Manifold Approximation and Projection; UMI, unique molecular identifier; VE, vascular endothelial cell.

were downregulated. In addition, several matrix metalloproteinases, such as *MMP1*, *MMP7*, *MMP9*, and *MMP10* ($log_2FC = -2.3, -1.9, -1.3$, and -2.0, respectively), were suppressed in GLPG3970-treated biopsies (Figure 3e).

Systemic treatment of patients with psoriasis with GLPG3970 in a phase 1b study revealed anti-inflammatory and antiproliferative effects at the transcriptome level

Because treatment with GLPG3970 effectively reduced key inflammatory psoriasis genes in an in vitro and ex vivo setting, next, the transcriptome of psoriatic lesions after in vivo treatment with GLPG3970 in the phase Ib study was analyzed (De Vos et al, 2026). Twenty-six patients participated in the respective study, with 23 patients (GLPG3970: n = 13; placebo: n = 10) completing the trial and providing skin biopsies at week 0 and week 6 for bulk RNA sequencing. Regarding these 23 final patients, the least squares mean PASI reduction at week 6 from baseline in the GLPG3970-treated patients amounted to 36.6% (±6.4) compared with 3.9% (±6.5) in the placebo group (Figure 4a) (De Vos et al, 2026). For transcriptome analysis, the 6 patients with the highest PASI score reduction from baseline (≥45%) were defined as "responders" and compared with the placebo-treated group adjusted for baseline. Gene set enrichment analysis of hallmark gene sets indicated a suppression of inflammation in the responder group (Figure 4b), with "IFN-γ response," "IFN-α response," "TNF signaling through NFKB," "IL-6 Jak singal transducer and activator of transcription 3 signaling," and "inflammatory response" (all adjusted $P < .0001$) being the 5 top downregulated pathways. In addition, proliferation- and metabolic-associated pathways such as "MYC targets V1," "E2F targets," "MTORC1 signaling," "P53 pathway" (all adjusted $P < .0001$), and "phosphoinositide 3-kinase protein kinase B mTOR signaling" (adjusted $P = .0005$) were suppressed by GLPG3970 treatment. The overall most downregulated differentially expressed genes included *CXCL8*, *DEFB4A*, *DEFB4B*, *IL1B*, and *CXCL1* ($log_2FC = -4.5, -3.8, -3.8, -3.6$, and -3.4, respectively) (Figure 4c). When looking at additional psoriasis-associated chemokines and cytokines, *IFNG*, *IL17A*, *IL17F*, *IL22*, *IL23A*, and *TNF* were not regulated, but *IL12B*, *IL19*, *IL20*, *CCL4*, and *CCL20* ($log_2FC = -1.8, -2.9, -3.0, -1.9$, and -2.2, respectively) and *CXCL1*, *CXCL9*, and *CXCL10* ($log_2FC = -3.4, -1.8$, and -1.6, respectively) were significantly suppressed in GLPG3970 responders versus in placebo-treated patients (Figure 4d). Among genes indicative of hyperproliferation and structural changes in psoriasis, *K6A*, *K16*, *SPRR2C*, and *SPRR2F* ($log_2FC = -2.2, -2.3, -2.5$, and -3.1, respectively) were downregulated, with late cornified envelope proteins and other small proline-rich proteins showing a tendency to

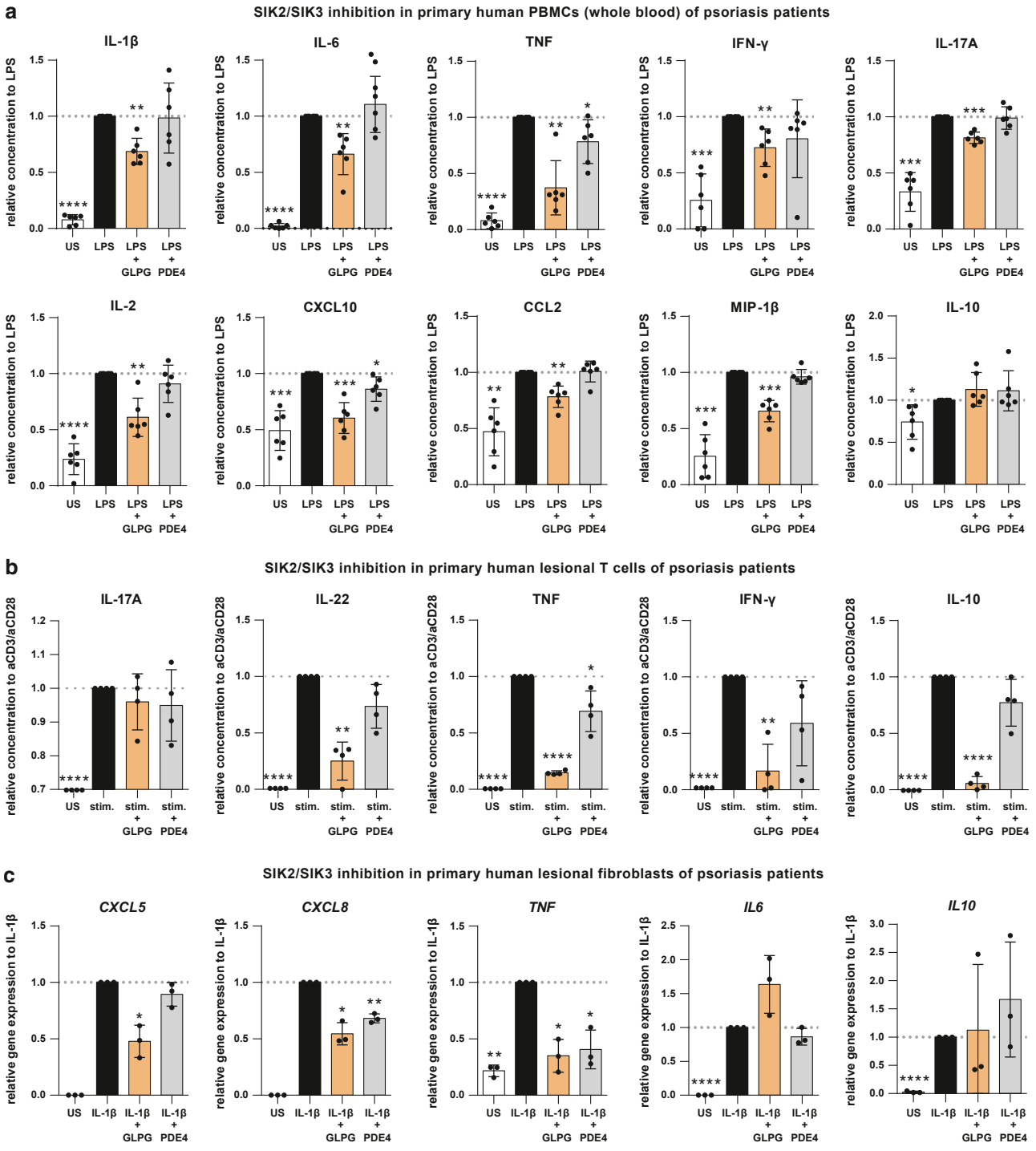


Figure 2. In vitro inhibition of SIK2 and SIK3 by GLPG3970 treatment reduces inflammation in primary human PBMCs (whole blood) as well as in lesional T cells and lesional fibroblasts from patients with psoriasis. (**a**) Whole blood of patients with psoriasis (n = 6) was preincubated with 10 μM GLPG3970 (denoted as GLPG), 5 μM apremilast (PDE4) or vehicle (DMSO 0.1%) for 30 min and then stimulated with 100 ng/mL of LPS for 2 h. The production of cytokines was analyzed by Bio-Plex Immunoassay of the supernatants. (**b**) Lesional T cells of patients with psoriasis (n = 4) were expanded for approximately 14 days before activation with αCD3/αCD28 (stim.) and 10 μM GLPG3970 (GLPG), 2 μM apremilast (PDE4), or vehicle (0.1% DMSO) for 48 h. Supernatant was analyzed with ELISA. (**c**) Lesional fibroblasts of patients with psoriasis (n = 3) were preincubated with 10 μM GLPG3970 (GLPG), 2 μM apremilast (PDE4), or vehicle (DMSO 0.1%) for 1 h and stimulated with 50 ng/ml of IL-1β overnight. RNA was extracted and analyzed by real-time qPCR. Comparison of treatment group to reference group (LPS, αCD3/αCD28 [stim.], or IL-1β) was performed using Welch's *t*-test. $*P \leq .05$, $**P \leq .01$, $***P \leq .001$, and $****P \leq .0001$. GLPG denotes GLPG3970 (SIK2/SIK3 inhibitor). stim. denotes stimulated (αCD3/αCD28), and US denotes unstimulated. h, hour; LPS, lipopolysaccharide; PDE4, phosphodiesterase 4; SIK, salt-inducible kinase.

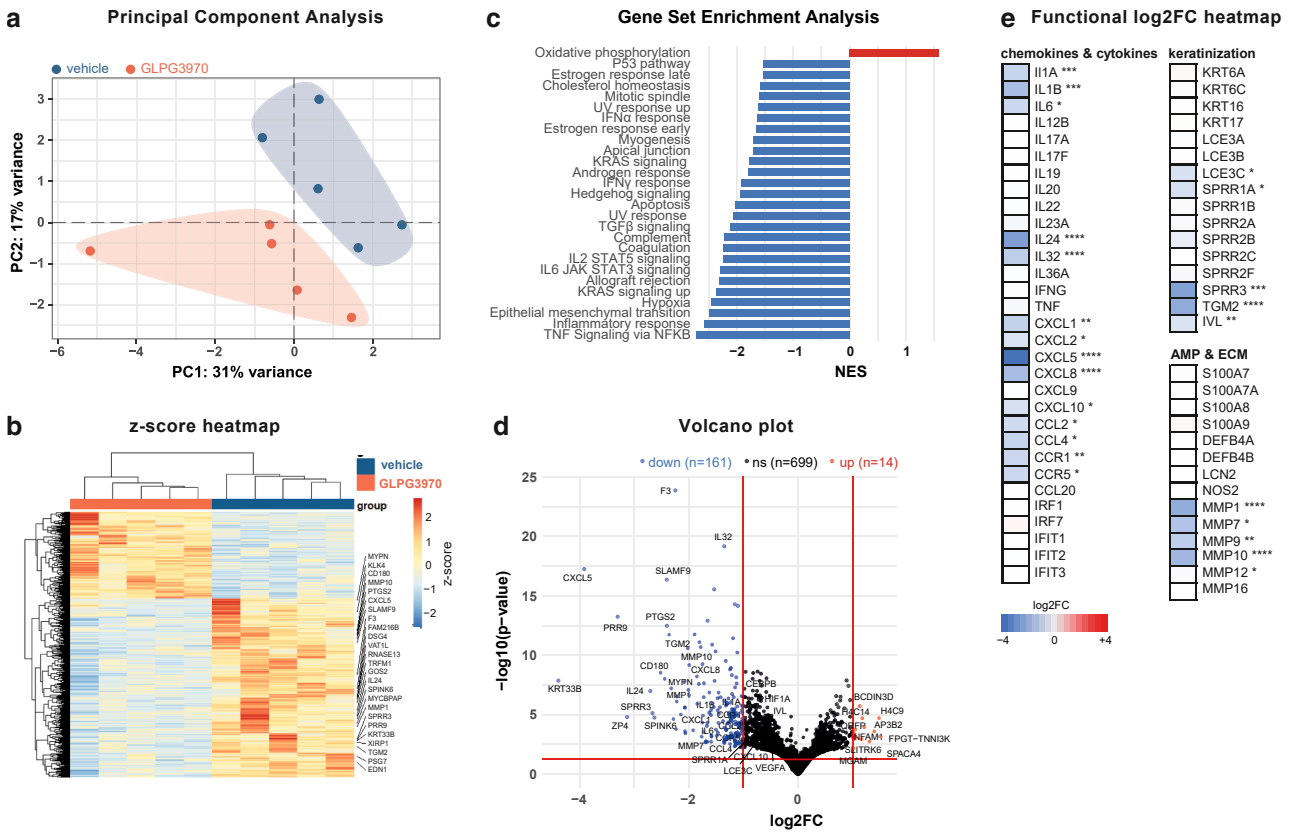


Figure 3. Blocking SIK2 and SIK3 ex vivo by GLPG3970 treatment reduced inflammation in psoriatic skin lesions. Punch biopsies 6 mm from psoriasis lesions (n = 5) were treated ex vivo with 100 μM GLPG3970 (orange) or vehicle (1% DMSO, blue) as control for 24 h. Subsequently, RNA was extracted and analyzed by bulk RNA sequencing. (**a**) PCA. (**b**) Heatmap of RNA-sequencing expression z-scores computed for differentially regulated genes (padj ≤ .05). Genes with $|\log_2 FC| \geq 2$ are labeled. (**c**) GLPG3970-suppressed (blue) and -activated (red) hallmark gene sets with padj ≤ .05 analyzed by fast gene set enrichment analysis compared with those of vehicle treated. (**d**) Volcano plot displaying differentially regulated genes analyzed with DESeq2 ($|\log_2 FC| \geq 1$, padj ≤ .05) between GLPG3970 and vehicle treated. Blue denotes GLPG3970 downregulated, red denotes GLPG3970 upregulated, and black denotes nonsignificant. (**e**) Functional heatmap of psoriasis-associated genes grouped in chemokines and cytokines, keratinization, and AMP and ECM shown as $\log_2 FC$ between GLPG3970 and vehicle treated analyzed with DESeq2. *$P \leq .05$, **$P \leq .01$, ***$P \leq .001$, and ****$P \leq .0001$. AMP, antimicrobial peptide; ECM, extracellular matrix; FC, fold change; h, hour; NES, normalized enrichment score; ns, nonsignificant; padj, adjusted *P*; PC, principal component; PCA, principal component analysis; SIK, salt-inducible kinase.

be suppressed. Regarding keratinocyte-derived antimicrobial peptides, *LCN2*, *DEFB4A*, and *DEFB4B* ($\log_2 FC = -1.7$, -3.8, and -3.8, respectively) were downregulated, with a strong trend for the S100A proteins. In addition, *NOS2* and the type I IFN-associated genes *IRF1*, *IRF7*, *IFIT1*, *IFIT2*, and *IFIT3* ($\log_2 FC = -2.7$, -0.8, -1.7, -1.5, -0.7, and -1.7, respectively) were suppressed.

Finally, the transcriptome from the ex vivo data (GLPG3970 vs vehicle treated) was compared with the in vivo data (GLPG3970 responders vs placebo at week 6) from the phase 1b study to identify common genes suppressed by GLPG3970. Here, 15 genes were significantly downregulated ($\log_2 FC \leq -0.58$) (adjusted $P \leq .05$ for ex vivo and $P \leq .05$ for in vivo) in both transcriptomes (Figure 4e). These shared genes included the cytokines and chemokines *IL1B*, *CXCL1*, *CXCL8*, *CXCL10*, and *CCL4* as well as the inflammatory receptors *ACKR2*, *TLR2*, and *ICOS*. Furthermore, the transcription factors *CEBPB* and *CEBPD* as well as *CD177* and *CLEC5A*, which are signature genes of neutrophils in inflammatory processes, were among these common GLPG3970-suppressed genes (Figure 4f).

DISCUSSION

The aim of the study presented in this paper was to assess SIK2/SIK3 inhibition through GLPG3970 in psoriasis disease–relevant cell types and in biopsies from patients. *SIK2* and *SIK3*, unlike *SIK1*, were both abundantly expressed in lesional psoriatic skin, and inhibition of SIK2/SIK3 ameliorated the acute phase and neutrophilic inflammation in the context of psoriasis in vitro, ex vivo, and in vivo.

SIK1, SIK2, and SIK3 molecules are found in all vertebrates with low human tissue specificity. SIK2 and SIK3 are constitutively expressed, unlike SIK1, which is rapidly upregulated by external stimuli such as high salt intake, membrane depolarization, or adrenocorticotropic hormone (Shi, 2024). However, little is known about the modulation of the expression levels of SIK2 and SIK3. Säll et al (2017) found mRNA levels to be downregulated in the white adipose tissue of individuals with obesity and to be negatively associated with insulin resistance. The data presented in this paper suggest that SIK2 and SIK3 are ubiquitously expressed in psoriasis, with SIK3 being even more prevalent in skin immune cells, such as MOs/Macs/DCs, T cells, and

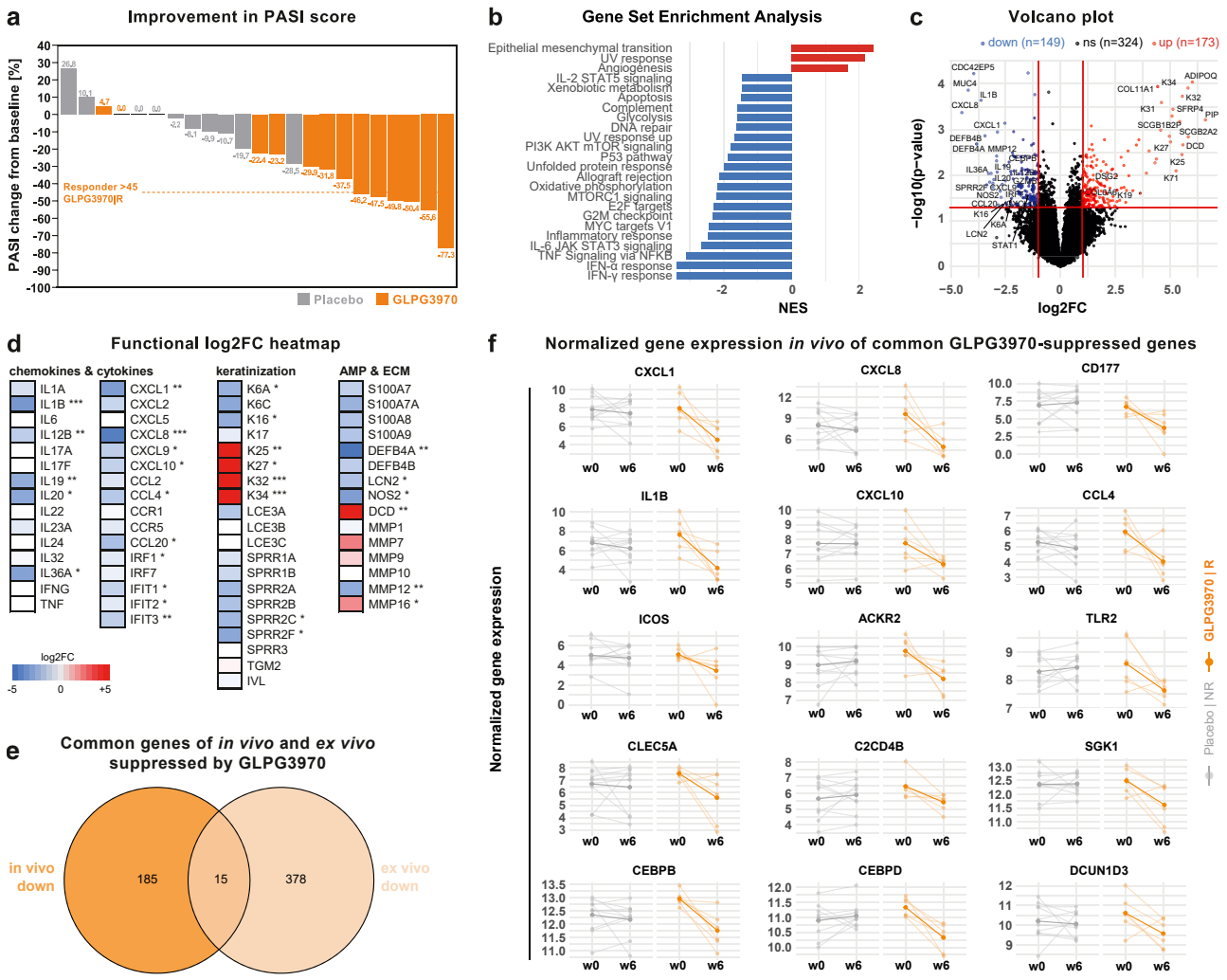


Figure 4. Effects of systemic treatment with GLPG3970 on the transcriptome of lesional skin of patients with psoriasis in a phase 1b study. A total of 23 patients with psoriasis completed the phase 1b study and received once-daily 350 mg GLPG3970 (orange, n = 13) or a placebo (gray, n = 10). Lesional skin biopsies from the participants of week 0 (denoted as w0, baseline) and week 6 (denoted as w6) were analyzed by bulk RNA sequencing. (**a**) Change in PASI scores at week 6 relative to that at baseline (week 0). Participants with PASI reduction ≥45% were considered responders (denoted as R). Downstream analyses were performed between GLPG3970 responders (n = 6) and placebo-treated patients (n = 10) at week 6, adjusted for baseline. (**b**) GLPG3970-suppressed (blue) and -activated (red) hallmark gene sets with padj ≤ .05 analyzed by fast gene set enrichment analysis in GLPG3970 responders versus placebo at week 6. (**c**) Volcano plot displaying differentially regulated genes analyzed with DESeq2 ($|\log_2FC| \geq 1$, $P \leq .05$) between GLPG3970 responders and placebo at week 6. Blue denotes GLPG3970 downregulated, red denotes GLPG3970 upregulated, and black denotes nonsignificant. (**d**) Functional heatmap of psoriasis-associated genes grouped in chemokines and cytokines, keratinization, and AMP and ECM shown as $\log_2FC$ between GLPG3970 responders and placebo at week 6, analyzed with DESeq2. (**e**) Intersection of genes downregulated by GLPG3970 between the in vivo phase 1b study (dark orange, GLPG3970 responders vs placebo at week 6, adjusted for baseline with $P \leq .05$ and $\log_2FC \leq -0.58$) and the ex vivo psoriatic skin culture from Figure 3 (light orange, GLPG3970 vs vehicle treated with padj ≤ .05 and $\log_2FC \leq -0.58$). In both studies, a total of 15 common genes were downregulated by GLPG3970. (**f**) Normalized gene counts for GLPG3970 responders and placebo-treated patients at week 0 (w0) and week 6 (w6) of the 15 identified GLPG3970-suppressed common genes of the in vivo and ex vivo study identified in **e**. *$P \leq .05$, **$P \leq .01$, and ***$P \leq .001$. R denotes GLPG3970 responder. AMP, antimicrobial peptide; ECM, extracellular matrix; FC, fold change; NES, normalized enrichment score; NR, nonresponder; ns, nonsignificant; padj, adjusted *P*.

keratinocytes, than SIK2. In general, SIK proteins undergo activation and inhibition primarily through phosphorylation. Consequently, mRNA expression levels are not a direct indicator of the catalytic function of SIK kinases in psoriasis but may serve as a hint. SIKs are activated by liver kinase B1 and inhibited by protein kinase A (Peixoto et al, 2024), and protein kinase A, in turn, is activated through an intracellular increase of cAMP. Protein kinase A activation by inhibition of cAMP degradation is the mode of action of phosphodiesterase 4 inhibitors, such as apremilast (Milakovic and Gooderham, 2021), indicating that blockage of this pathway indeed results in the suppression of psoriasis. A strong and broad downregulation of psoriasis-associated genes was observed in PBMCs, T cells, and fibroblasts by GLPG3970. Nevertheless, the aforementioned induction of IL-10 could not be detected (Peixoto et al, 2024). This could be due to overall low detection levels of IL-10 in PBMCs in the Bio-Plex Immunoassay and/or due to different time points, for example, in the fibroblast analysis. *IL10* mRNA is rapidly degraded, rendering high chances that the optimal induction window was missed (Grant et al, 2008). In addition, it remains questionable to what extent an increase in IL-

10 is of clinical importance in the therapeutic setting of psoriasis. Although IL-10–deficient mice develop more severe psoriasis than wild-type mice, and *IL10* mRNA levels are decreased in psoriatic skin, a placebo-controlled clinical trial in 2002 exploring subcutaneous IL-10 administration in patients with psoriasis missed its primary endpoint, with no difference in PASI reduction after 12 weeks (Asadullah et al, 1998; Jin et al, 2018; Kimball et al, 2002). In this study, IL-1β– or IL-17A–stimulated GLPG3970-treated keratinocytes showed neither a downregulation of proinflammatory cytokines nor an upregulation of SIK-response genes, such as *VEGFA*, *EREG*, and *NR4A2*, suggesting that direct SIK2/SIK3 inhibition does not play a major role in keratinocytes. SIK2 and SIK3 are highly expressed in psoriatic keratinocytes (Figure 1), but transcript abundance does not necessarily reflect catalytic activity or functional dependence in a given cell type. Accordingly, the lack of effect of SIK inhibition in keratinocytes is best interpreted from the absent functional response rather than from expression levels. Interestingly, it has been shown that phosphodiesterase 4 inhibitors also have cell lineage–specific effects. Kataoka et al (2020) observed that downregulation of proinflammatory cytokines in apremilast-treated keratinocytes but not in PBMCs was due to deactivation of the MEK/ERK pathway. This was independent of intracellular cAMP elevations and, therefore, also independent of SIK (Kataoka et al, 2020). Comprehensive transcriptome analysis of full lesional biopsies exposed to GLPG3970 for 24 hours revealed expression patterns that correlated with in vitro findings. Psoriasis signature genes and acute-phase inflammatory signals such as *CXCL1*, *CXCL5*, *CXCL8* or *IL1B*, *IL6*, and *IL24* were downregulated, with a focus on MO/Mac/DC- and neutrophil-associated genes, such as *CXCL2*, *CCL2*, and *CCL4*, along with the CCL4 receptors *CCR1* and *CCR5* or the MO/Mac-derived matrix metalloproteinases *MMP7*, *MMP9*, *MMP10*, and *MMP12* (Sieminska et al, 2024; Mezentsev et al, 2014; Zhou et al, 2023). However, marker genes related to epidermal differentiation (*K6*, *K16*, *K17*) and antimicrobial peptides (*S100A7*, *S100A8*, *S100A9*, *DEFB4A*, *DEFB4B*) remained largely unchanged. These findings align with the proposed mechanism of action of SIK2/SIK3 inhibition, which closely parallels that of apremilast. Apremilast primarily reduces the infiltration and/or inflammatory cytokine production of MOs/Macs/DCs, neutrophils, and T cells (Schafer et al, 2014; Schett et al, 2010), suggesting mainly subsequent effects on keratinocytes. In addition, today, disease modification is a key aim of psoriasis treatment. This concept promotes early intervention in the inflammatory cascade to reduce the number of pathogenic tissue-resident memory T cells, which are responsible for the re-emergence of psoriatic lesions after cessation of treatment (Eyerich et al, 2021). Therefore, therapeutic targeting of DCs, as the stimulating cell group of T cells, seems crucial.

When analyzing the transcriptome of skin biopsies from responders versus placebo-treated patients in the phase 1b study, the group of downregulated genes included key psoriasis genes related to epidermal differentiation (*K6A*, *K6C*, *K16*, *K17*) and antimicrobial peptides (*LCN2*, *DEFB4A*, *DEFB4B*), reflecting the secondary impact of SIK2/SIK3 inhibition in keratinocytes that becomes apparent after several days or weeks of continuous treatment. The 15 genes that were downregulated in both the ex vivo and in vivo contexts may serve as stable marker genes for SIK2/SIK3 inhibition in psoriasis because they are efficiently suppressed in early (ex vivo) and late (in vivo) stages of treatment. Regarding these genes, a previous focus on genes related to initial inflammatory signals of the MO/Mac/DC compartment with subsequent inhibition of Th1/Th17 development or recruitment is apparent. For example, IL-1β is mainly produced by Macs, DCs, and keratinocytes, leading to Th17 cell differentiation, proliferation of γδ T cells, DC clusters, and stimulation of keratinocytes (Sieminska et al, 2024; Cai et al, 2019). Signaling through toll-like receptor 2 in MOs and keratinocytes also promotes the development of Th1/Th17 cells, and CCL4 leads to the recruitment of DCs, MOs, and Th1 cells through its receptors CCR1 and CCR5 (Sun et al, 2019; Nedoszytko et al, 2014). Nevertheless, when analyzing these common genes, an equally strong neutrophil-associated aspect becomes visible. CXCL1, CXCL8, and CD177 are important indicators of neutrophilic infiltration, with CXCL1 and CXCL8 being the main chemotactic factors in psoriasis and $CD177^{+}$ neutrophils preferentially migrating into sites of inflammation (Sieminska et al, 2024; Zheng et al, 2024). Furthermore, CEBPB is not only vital for MOs and Macs and their involvement in Th17 priming but also for cytokine production in mature neutrophils (Cloutier et al, 2009; Simpson-Abelson et al, 2017; Wu et al, 2024). CLEC5A, produced by MOs, Macs, DCs, and neutrophils, is needed for the development and maturation of $IL\text{-}17A^{+}$–producing neutrophils in IL-23–mediated inflammatory skin diseases (Furuya et al, 2024; Sung et al, 2020). This emphasis on neutrophils is also seen with apremilast and its successful application in a variety of neutrophilic diseases, such as palmoplantar pustulosis or Behçet's disease; for the latter, apremilast is even officially approved in the United States and Europe. Concerning palmoplantar pustulosis, a randomized, placebo-controlled study showed a Palmoplantar Pustulosis Area and Severity Index 50 of 78.3% and Palmoplantar Pustulosis Area and Severity Index 75 of 43.5% after 16 weeks of 30 mg apremilast twice daily (Terui et al, 2023). In comparison, in similar trials, Palmoplantar Pustulosis Area and Severity Index 75 was reached in 26.6% with secukinumab and in 20.4% with guselkumab (Mrowietz et al, 2019; Terui et al, 2019). This indicates that not only apremilast but also SIK2/SIK3 inhibitors could be an effective therapeutic means in neutrophilic/pustular diseases, which still remain particularly hard to treat.

There are several limitations to this study. First, SIK expression was only characterized at the mRNA level, and no protein or phosphorylation/kinase-activity data were obtained. Second, concentrations used for apremilast treatment in keratinocytes, fibroblasts, and T cells might have been too low. However, in the literature, 1.0 μM of apremilast has been used successfully in keratinocytes (Schafer et al, 2010), and half-maximal inhibitory concentration determination in αCD3/αCD28-activated human PBMCs suggested that 2 μM would be sufficient in T cells (Supplementary Table S1). Furthermore, GLPG3970 has a limited off-target effect on RIPK2 (Peixoto et al, 2024). Inhibition of RIPK2, such as that of RIPK3, has been shown to alleviate inflammatory diseases

(Haile et al, 2019; Huang et al, 2022), rendering it possible that the anti-inflammatory effect in psoriasis reported in this paper is partly due to RIPK2 inhibition. Nevertheless, Peixoto et al (2024) showed that GLPG3970 is 10-fold more potent on SIK2 and 20-fold more potent on SIK3 than on RIPK2, indicating high selectivity for SIK2 and SIK3. Concerning the analysis of the transcriptome of responders versus placebo-treated patients in the clinical phase 1b study, the 6 patients with the highest PASI response were defined as the "responder group." This was a rather artificial segregation, but for the transcriptome analyses, a homogeneous cohort was necessary, given the small total number of participants.

In summary, this study provides in-depth insight into the mode of action of SIK2/SIK3 inhibition by GLPG3970 in psoriatic inflammation, with direct effects on the MOs/Mac/DCs and the T-cell compartment and subsequent effects on keratinocytes. Furthermore, neutrophil-associated inflammation is efficiently downregulated, suggesting that GLPG3970 might not only be effective in psoriasis but also in pustular skin diseases.

MATERIALS AND METHODS

Spatial transcriptomics

Spatial transcriptomics data were derived from previous work by our group. Patient characteristics and data analysis are described previously (Schäbitz et al, 2022). In total, 9 patients with psoriasis (lesional = 9; nonlesional = 3) were used for *SIK* expression analysis.

Single-cell RNA sequencing

Psoriatic punch biopsies of 6 mm (n = 7) were digested for 3 hours to isolate skin cells using the Whole Skin Dissociation Kit (130-101-540) and gentleMACS Dissociator (program h_skin_01_01) from Miltenyi according to the manufacturer's instructions. After cell sorting with a FACSAria Fusion (BD Biosciences), living (propidium iodide$^-$) immune (CD45$^+$) and epithelial (CD45$^-$) cells were mixed in an equal ratio. A total of 24,000 cells per biopsy were used for GEM generation and library preparation using the Chromium Next GEM Single Cell 3′ Reagent Kits (10x Genomics) in combination with dual indexes according to the manufacturer's instructions. Samples were sequenced on a NovaSeq 6000 as paired-end reads with 28-10-10-90 cycles and a sequencing depth of at least 20,000 read pairs per cell. Sequence alignment was performed using the STAR aligner with the human genome reference hg38. Ambient RNA contamination was removed using CellBender (Fleming et al, 2023). Quality control was performed with scanpy (Wolf et al, 2018), retaining cells with 500–100,000 unique molecular identifiers; at least 100 detected genes; and a mitochondrial gene fraction $\leq$ 25%. Genes detected in more than 20 cells with $\geq$1 unique molecular identifier count were retained. Doublets were identified and removed using Scrublet (Wolock et al, 2019), assuming a doublet rate of 0.1. Raw count data were obtained from the publicly available dataset from Reynolds et al (2021). During quality control, cells were retained if they contained more than 250 genes; 500–400,000 unique molecular identifiers; a ribosomal gene fraction between 5 and 60%; a mitochondrial gene fraction $\leq$25%; and a Scrublet score $\leq$ 0.6. For downstream analysis, data were normalized using size factors derived from coarse Leiden clustering (resolution = 0.1) and log transformed, and 4,000 highly variable genes were selected. Cell cycle states were scored with scanpy (cell_cycle_score (Macosko et al, 2015)), and batch effects were corrected with scVI (Lopez et al, 2018). Dimensionality reduction was performed using principal component analysis (n = 7 components), followed by the construction of a neighborhood graph (n_neighbors = 15). Uniform Manifold Approximation and Projection was used for visualization (McInnes et al, 2020[1]).

For cell type transfer, we used the scANVI (Xu et al, 2021) model, a semisupervised variational autoencoder. We defined the quality-controlled lesional and nonlesional psoriasis samples from Reynolds et al (2021) as the reference and our single-cell dataset as the query. Before training the scANVI model, both datasets were concatenated using sample_names as the batch key. The combined dataset was normalized (normalize_total, target_sum = 1e4) and log transformed, and 2000 highly variable genes were selected using the cell_ranger flavor. Cells assigned to the unlabeled_category were annotated as "unknown." Finally, the scANVI model was trained using default parameters. To ensure adequate representation of rare cell types, including plasma cells, the n_samples_per_label parameter was set to 79. The trained scANVI model was used to learn a joint latent representation of the reference and query data and to transfer 42 cell types from the reference to the query dataset. The 42 subtypes from Reynolds et al (2021) were summarized into 9 major cell-type groups, that is, T cells, MOs/Mac/DCs, vascular endothelial cells, lymphatic endothelial cells, KCs, fibroblasts, pericytes, melanocytes, and mast cells.

Compounds

GLPG3970 is a selective SIK2/SIK3 inhibitor whose development has been extensively described (Peixoto et al, 2024). Apremilast (CAS: 608141-41-9) is a commercially available drug purchased from Matrix Scientific (catalog reference number 116180). Both compounds were dissolved in 100% DMSO. Half-maximal inhibitory concentration values were calculated on human MOs, human MO-derived Macs, and PBMCs, which were stimulated for 24 hours with the compounds. Cytokine readouts, including TNF, IL-12, and IL-2, were quantified using custom-developed ELISA protocols optimized for sensitivity and specificity (capture and detection antibodies from R&D Systems and BD Pharmingen), with half-maximal inhibitory concentration values reported in Supplementary Table S1. On the basis of a half-maximal inhibitory concentration of 240 nM in LPS-stimulated MO-derived Macs, near-maximal TNF suppression was observed between 2.5 and 20 μM; a concentration of 10 μM was therefore selected for GLPG3970 in the in vitro assays.

Whole blood assay

Sample collection and the assay were performed as previously described (Peixoto et al, 2024). In brief, 3 ml of blood from 6 patients with psoriasis was collected. From each patient, 200 μl of blood was preincubated in duplicate with 10 μM GLPG3970 or 5 μM apremilast or with vehicle (0.1% DMSO) for 30 minutes at 37 °C, 5% carbon dioxide in 96-well plates. Then, blood cells were stimulated with 100 ng/ml LPS (InvivoGen) or left unstimulated for 2 hours at 37 °C, 5% carbon dioxide. Supernatants were collected, and concentrations of cytokines were measured with the Bio-Plex Pro Human Cytokine 27-plex Assay kit (Bio-Rad Laboratories) according to the manufacturer's instructions.

[1] McInnes L, Healy J, UMAP MJ. Uniform manifold approximation and projection for dimension reduction. arXiv 2020.

GLPG3970 treatment of lesional T cells

T cells were extracted from psoriatic skin lesions (n = 4) as described in detail by Lauffer et al (2018). Frozen T cells were thawed and stimulated with αCD3 (precoated in PBS) and αCD28 (soluble) (each 0.75 μg/ml, BD Bioscience) for 48 hours at 37 °C, 5% carbon dioxide in T-cell media (RPMI 1640 medium supplemented with 5% human serum, 0.1 mM nonessential amino acids, 2 mM L-glutamine, 1 mM sodium pyruvate, 100 U/ml penicillin/streptomycin [all from Gibco]) as well as 60 U/ml IL-2 (Proleukin, Novartis). T cells were expanded for a total of 2 weeks in the presence of 60 U/ml IL-2 in T-cell medium. The medium was exchanged 3 times a week. Expanded T cells (1.5×10^6 cells/ml) were activated with αCD3/αCD28 in the presence of 10 μM GLPG3970 or 2 μM apremilast or with vehicle (0.1% DMSO) for 48 hours at 37 °C, 5% carbon dioxide. The supernatant was collected, and cytokine concentrations of TNF (R&D Systems, DY210), IL-17A (R&D Systems, DY317), IL-22 (R&D Systems, DY782), IFN-γ (R&D Systems, DY285B), and IL-10 (R&D Systems, DY217B) were analyzed by ELISA according to the manufacturer's instructions.

GLPG3970 treatment of fibroblasts

Fibroblasts were isolated from skin biopsies of patients with psoriasis (n = 3) as previously described (Lavazais et al, 2023). Fibroblasts were cultivated until 60–80% confluence was reached and then 3 hours of starvation (DMEM medium without fetal calf serum), followed by a 1-hour preincubation with 10 μM GLPG3970, 2 μM apremilast, or vehicle (0.1% DMSO). Cells were stimulated with recombinant human IL-1β (50 ng/ml; PromoCell) for 16 hours at 37 °C, 5% carbon dioxide in the presence of the test compounds. Changes in gene expression level were analyzed by real-time qPCR.

Real-time qPCR

RNA from fibroblasts and keratinocytes was extracted with the RNeasy Mini Plus Kit (Qiagen) and transcribed into cDNA using the High-Capacity cDNA Reverse Transcript Amplification Kit (Applied Biosystems), according to the manufacturer's instructions. Real-time PCR was performed using Fast Start SYBR Green Master Mix (Roche) with the ViiA7 Real-Time PCR machine (Applied Biosystems). Primers for the genes of interest were designed using National Center for Biotechnology Information Primer Blast and synthesized by Metabion. Primer sequences are listed in Supplementary Table S2. Gene expression was normalized to the housekeeping gene *18S*, and expression results were analyzed with the $2^{-\Delta\Delta CT}$ method.

Ex vivo skin biopsy treatment with GLPG3970 and sequencing

Treatment. Punch biopsies of 6 mm were obtained from the lesional skin of patients with psoriasis (n = 5). Biopsies were divided into 2 parts and cultured in RPMI 1640 (Gibco) with 1% human serum (Sigma-Aldrich, catalog number H4522-100ML), 0.1 mM MEM-nonessential amino acid, 2 mM l-glutamine, 1 mM sodium pyruvate, and penicillin/streptomycin (100 U/ml) (all from Gibco). One part of the biopsy was stimulated with 100 μM GLPG3970 (a 10-fold concentration of the in vitro experiments as described in Lavazais et al (2023)), and the other part was stimulated with vehicle (1% DMSO) for 24 hours. Thereafter, biopsies were stored in RNAprotect Tissue Reagent (Qiagen) at −80 °C until RNA was isolated using QIAzol Lysis Reagent (Qiagen) and the miRNeasy Mini Kit (Qiagen) according to the manufacturer's instructions.

Sequencing. RNA-sequencing libraries were generated using the TruSeq Stranded Total RNA Kit (Illumina) according to the manufacturer's high sample instructions and sequenced on an Illumina HiSeq4000 (paired-end, 2 × 150 bp, ∼40 Mio reads per sample and end).

Processing and analysis. Sequence alignment was performed using the STAR aligner with the human genome reference hg38. Raw count data for 60,666 genes were processed using the DESeq2 R package, version 1.32.0 (Love et al, 2014). First, a variance stabilizing transformation was applied to normalize the data. Genes not annotated as protein coding and genes with a total count <1 across all samples were removed. To assess global expression patterns, principal component analysis was conducted on the normalized dataset. Differential gene expression analysis was performed using DESeq2 (Love et al, 2014), applying Benjamini–Hochberg correction (Benjamini and Hochberg, 1995) for multiple testing. Age was included as a covariate in the model to account for biological variance, using the following design formula: Yg ∼ age + group, where Yg is the raw count of gene g. Differentially expressed genes were defined using a threshold for the false discovery rate–adjusted $P \leq .05$. The heatmap was generated using the pheatmap package, version 1.0.12 (GitHub, 2018). Fast gene set enrichment analysis is described in the following section.

Psoriasis phase 1b study with GLPG3970 and sequencing

Study. GLPG3970 was evaluated in a short phase 1b study in patients with psoriasis. Twenty-six patients with moderate-to-severe psoriasis were randomized for the study and treated with 350 mg GLPG3970 once daily compared with placebo in a 3:2 ratio (De Vos et al, 2026). The median age was 44.0 (minimum: 24; maximum: 62) years in the treatment group and 36.0 (minimum: 23; maximum: 47) years in the placebo group, with 9 (60%) and 5 (45.5%) males, respectively. Disease duration was 12.8 (minimum: 5; maximum: 37) years in the treatment arm and 16.8 (minimum: 5; maximum: 33) years in the placebo arm. The median PASI score at baseline was 15.6 (minimum: 12.2; maximum: 58.0; treatment group) and 16.1 (minimum: 12.7; maximum: 30.8; placebo group) (De Vos et al, 2026). Further study information is provided in previous work (De Vos et al, 2026) and on ClinicalTrials.gov (identification NCT04106297). Two of 15 patients in the treatment arm and 1 of 11 in the placebo group discontinued the study. Punch biopsies for transcriptomics were obtained from lesional and previously lesional skin at weeks 0 and 6 from the remaining 23 patients.

Sequencing. Total RNA was obtained using a RNeasy kit following the manufacturer's instructions (Qiagen, Venlo, The Netherlands). Illumina sequencing libraries were prepared using polyA capture (mRNA + long noncoding RNA), multiplexed for each tissue, and processed on an Illumina NovaSeq 6000 sequencer.

Processing and analysis. Reads were mapped to the human reference transcriptome (hg38 build v100, Ensembl version; primary assembly) using the pseudoalignment model with Kallisto 0.43.1 (Bray et al, 2016). Differential gene expression analysis was performed using the R package DESeq2, version 1.32.0 (Love et al,

2014). The estimated number of reads obtained from Kallisto was used as the input for DESeq2. Briefly, DESeq2 normalizes samples according to per-sample sequencing depth and accounts for intra-sample variability. Then, it fits data to a negative binomial generalized linear model and calculates the Wald statistic. Finally, the raw *P*-values were corrected using the false discovery rate for multiple testing by the Benjamini–Hochberg method. Functional enrichment was evaluated using fast gene set enrichment analysis (Korotkevich et al, 2016[2]), on the basis of the full list of differentially expressed genes that were ranked by the Wald test results and using the MSigDB (Molecular Signatures Database) as the reference (Liberzon et al, 2011). The selected MSigDB gene set was hallmark.

Statistical analyses

Data were analyzed using descriptive statistics, including mean and SD, and unpaired *t*-test with Welch's correction to assess significance. Significance levels were defined as $*P \leq .05$, $**P \leq .01$, $***P \leq .001$, and $****P \leq .0001$. Data analysis and processing were performed using GraphPad Prism 10 software, and figures were generated using Microsoft PowerPoint and Adobe Illustrator CS6.

ETHICS STATEMENT

Human skin samples (punch biopsies) and blood-derived cells for the in vitro and ex vivo experiments were obtained from patients enrolled in the Biobank Biederstein after obtaining written informed consent. The study was conducted in accordance with the Declaration of Helsinki and was approved by the Ethics Committee of the Technical University of Munich (44/16S and 5590/12). Human skin samples for the in vivo analyses were acquired as part of a phase 1b study in patients with psoriasis (NCT04106297, part 4); further details are provided in De Vos et al (2026). The study was approved by an ethics committee at each study site (Antwerp, Belgium: SGS Clinical Pharmacology Unit Antwerp [ZNA Stuivenberg]; Chisinau, Moldova: Clinical Republican Hospital, Arsensia Experimental Medicine; Kyiv, Ukraine: Medical Center Harmoniia Krasy, Department of Clinical Trials) and was conducted in accordance with the International Council for Harmonization Good Clinical Practice guidelines, the Declaration of Helsinki, and applicable local laws and regulations. All patients provided written informed consent before enrolling in the study.

DATA AVAILABILITY STATEMENT

Datasets related to this article are publicly available at Gene Expression Omnibus (https://www.ncbi.nlm.nih.gov/geo/query/acc.cgi) under the following accession numbers: GSE206391 (spatial transcriptomics; https://www.ncbi.nlm.nih.gov/geo/query/acc.cgi?acc=GSE206391), GSE313454 (single-cell RNA sequencing; https://www.ncbi.nlm.nih.gov/geo/query/acc.cgi?acc=GSE313454), GSE328285 (bulk RNA sequencing of the ex vivo biopsies; https://www.ncbi.nlm.nih.gov/geo/query/acc.cgi?acc=GSE328285), and GSE331382 (bulk RNA sequencing of the phase 1b study, in vivo biopsies; https://www.ncbi.nlm.nih.gov/geo/query/acc.cgi?acc=GSE331382).

ORCID

Anna Caroline Pilz: http://orcid.org/0000-0002-3028-4556

CONFLICT OF INTEREST

ACP received consulting and/or speaker's fees and/or travel grants from Abbvie, ALK-Abelló, Bristol Myers Squibb, Boehringer Ingelheim, LEO Pharma, Novartis, and UCB. MC was an employee of Galapagos at the time of the work. SL was an employee of Galapagos at the time of the work. TB has received speaker and consultancy fees and has received institutional research grants from Alk-Abelló, Amgen, Almirall, Celgene, Eli Lilly, Galderma, LEO Pharma, Mylan, Novartis, Phadia-Thermo-Fisher, Regeneron, Sanofi-Genzyme, and Viatris. FL is a member of advisory boards and/or a speaker for AbbVie, Almirall, Amgen, Biogen, Boehringer Ingelheim, Bristol Myers Squibb, Hexal, Incyte, Janssen, LEO Pharma, Lilly, Novartis, Pfizer, Roche, Sanofi, UCB, and Union Therapeutics. KE is an advisory board member or speaker for Abbvie, Almirall, Boehringer Ingelheim, BMS, Leo, Lilly, Janssen, Galderma, Novartis, Pfizer, Sanofi, and UCB. SDV is employee of Galapagos. The remaining authors state no conflict of interest.

[2] Korotkevich G, Sukhov V, Budin N, Shpak B, Artyomov MN, Sergushichev A. Fast gene set enrichment analysis. bioRxiv 2016.

ACKNOWLEDGMENTS

Editorial and publications management support was provided by PharmaGenesis London (London, United Kingdom) and was funded by Galapagos NV (Mechelen, Belgium). The work was funded by Galapagos NV. Parts of the study were performed with samples from the Biobank Biederstein of the Technical University of Munich, which was supported by the European Research Council (IMCIS 676858), German Research Foundation (EY97/3-1), and the Helmholtz Association (''Impuls- und Vernetzungsfonds''). Furthermore, projects of FL and TB received funds from the German Research Foundation (RTG2668) (project A2 to TB and A3 to FL; project-ID: 435874434).

AUTHOR CONTRIBUTIONS

Conceptualization: ACP, FL, KE, SDV, MJ; Data Curation: ACP, EB, SL, MC, CH, MJ; Formal Analysis: ACP, EB, SL, MC, CH, MJ; Funding Acquisition: MPM, TB, KE, SDV; Investigation: ACP, SL, EB, CH, MJ; Methodology: ACP, CH, EB, MC, KE, SDV, MJ; Project Administration: KE, SDV; Resources: MPM, TB, KE, SDV; Supervision: CH, MPM, TB, KE, SDV, MJ; Visualization: ACP, EB, MC, CH; MJ; Writing – Original Draft Preparation: ACP, EB, MC, KE, SDV, MJ; Writing – Review and Editing: ACP, EB, MC, CH, SL, MPM, TB, FL, KE, SDV, MJ

DECLARATION OF GENERATIVE ARTIFICIAL INTELLIGENCE (AI) OR LARGE LANGUAGE MODELS (LLMs)

The author(s) did not use AI/LLM in any part of the research process and/or manuscript preparation.

SUPPLEMENTARY MATERIAL

Supplementary material is linked to the online version of the paper at www.jidonline.org, and at 10.1016/j.jid.2026.07.033.

REFERENCES

Armstrong AW, Gooderham M, Warren RB, Papp KA, Strober B, Thaçi D, et al. Deucravacitinib versus placebo and apremilast in moderate to severe plaque psoriasis: efficacy and safety results from the 52-week, randomized, double-blinded, placebo-controlled phase 3 POETYK PSO-1 trial. J Am Acad Dermatol 2023;88:29–39.

Armstrong AW, Mehta MD, Schupp CW, Gondo GC, Bell SJ, Griffiths CEM. Psoriasis prevalence in adults in the United States. JAMA Dermatol 2021;157:940.

Asadullah K, Sterry W, Stephanek K, Jasulaitis D, Leupold M, Audring H, et al. IL-10 is a key cytokine in psoriasis. Proof of principle by IL-10 therapy: a new therapeutic approach. J Clin Invest 1998;101:783–94.

Babbe H, Sundberg TB, Tichenor M, Seierstad M, Bacani G, Berstler J, et al. Identification of highly selective SIK1/2 inhibitors that modulate innate immune activation and suppress intestinal inflammation. Proc Natl Acad Sci USA 2024;121:e2307086120.

Benjamini Y, Hochberg Y. Controlling the false discovery rate: a practical and powerful approach to multiple testing. J R Stat Soc B 1995;57:289–300.

Bray NL, Pimentel H, Melsted P, Pachter L. Near-optimal probabilistic RNA-seq quantification [published correction appears in Nat Biotechnol 2016;34:888]. Nat Biotechnol 2016;34:525–7.

Cai Y, Xue F, Quan C, Qu M, Liu N, Zhang Y, et al. A critical role of the IL-1β-IL-1R signaling pathway in skin inflammation and psoriasis pathogenesis. J Invest Dermatol 2019;139:146–56.

Cloutier A, Guindi C, Larivée P, Dubois CM, Amrani A, McDonald PP. Inflammatory cytokine production by human neutrophils involves C/EBP transcription factors. J Immunol 2009;182:563–71.

De Vos S, Desroy N, Bellaire SJ, Fernandes AP, Lavazais S, Merciris D, et al. Selective SIK2/SIK3 inhibition reprograms pro- and antiinflammatory pathways in myeloid cells, improving autoimmune disease outcomes. JCI Insight 2026;11:e171776.

Eyerich K, Weisenseel P, Pinter A, Schäkel K, Asadullah K, Wegner S, et al. IL-23 blockade with guselkumab potentially modifies psoriasis pathogenesis: rationale and study protocol of a phase 3b, randomised, double-blind, multicentre study in participants with moderate-to-severe plaque-type psoriasis (GUIDE). BMJ Open 2021;11:e049822.

Fleming SJ, Chaffin MD, Arduini A, Akkad AD, Banks E, Marioni JC, et al. Unsupervised removal of systematic background noise from droplet-based single-cell experiments using CellBender. Nat Methods 2023;20:1323–35.

Furuya H, Nguyen CT, Chan T, Marusina AI, Merleev AA, Garcia-Hernandez ML, et al. IL-23 induces CLEC5A+ IL-17A+ neutrophils and

elicit skin inflammation associated with psoriatic arthritis. J Autoimmun 2024;143:103167.

Garzorz-Stark N, Lauffer F, Krause L, Thomas J, Atenhan A, Franz R, et al. Toll-like receptor 7/8 agonists stimulate plasmacytoid dendritic cells to initiate TH17-deviated acute contact dermatitis in human subjects. J Allergy Clin Immunol 2018;141:1320–33.e11.

Grant LR, Yao ZJ, Hedrich CM, Wang F, Moorthy A, Wilson K, et al. Stat4-dependent, T-bet-independent regulation of IL-10 in NK cells. Genes Immun 2008;9:316–27.

Haile PA, Casillas LN, Votta BJ, Wang GZ, Charnley AK, Dong X, et al. Discovery of a first-in-class Receptor Interacting Protein 2 (RIP2) Kinase Specific Clinical Candidate, 2-((4-(Benzo[d]-thiazol-5-ylamino)-6-(tert-butylsulfonyl)-quinazolin-7-yl)oxy)ethyl dihydrogen phosphate, for the treatment of inflammatory diseases. J Med Chem 2019;62:6482–94.

Huang D, Chen P, Huang G, Sun H, Luo X, He C, et al. Salt-inducible kinases inhibitor HG-9-91-01 targets RIPK3 kinase activity to alleviate necroptosis-mediated inflammatory injury. Cell Death Dis 2022;13:188.

Jin SP, Koh SJ, Yu DA, Kim MW, Yun HT, Lee DH, et al. Imiquimod-applied interleukin-10 deficient mice better reflects severe and persistent psoriasis with systemic inflammatory state. Exp Dermatol 2018;27:43–9.

Kataoka S, Takaishi M, Nakajima K, Sano S. Phosphodiesterase-4 inhibitors reduce the expression of proinflammatory mediators by human epidermal keratinocytes independent of intracellular cAMP elevation. J Dermatol Sci 2020;100:230–3.

Kimball AB, Kawamura T, Tejura K, Boss C, Hancox AR, Vogel JC, et al. Clinical and immunologic assessment of patients with psoriasis in a randomized, double-blind, placebo-controlled trial using recombinant human interleukin 10. Arch Dermatol 2002;138:1341–6.

GitHub. pheatmap: Pretty heatmaps. R package version 1.0.12 2018. https://github.com/raivokolde/pheatmap 2018 (accessed January 7, 2026).

Lauffer F, Jargosch M, Krause L, Garzorz-Stark N, Franz R, Roenneberg S, et al. Type I immune response induces keratinocyte necroptosis and is associated with interface dermatitis. J Invest Dermatol 2018;138:1785–94.

Lavazais S, Jargosch M, Dupont S, Labéguère F, Menet C, Jagerschmidt C, et al. IRAK4 inhibition dampens pathogenic processes driving inflammatory skin diseases. Sci Transl Med 2023;15:eabj3289.

Liberzon A, Subramanian A, Pinchback R, Thorvaldsdóttir H, Tamayo P, Mesirov JP. Molecular signatures database (MSigDB) 3.0. Bioinformatics 2011;27:1739–40.

Lopez R, Regier J, Cole MB, Jordan MI, Yosef N. Deep generative modeling for single-cell transcriptomics. Nat Methods 2018;15:1053–8.

Love MI, Huber W, Anders S. Moderated estimation of fold change and dispersion for RNA-seq data with DESeq2. Genome Biol 2014;15:550.

Macosko EZ, Basu A, Satija R, Nemesh J, Shekhar K, Goldman M, et al. Highly parallel genome-wide expression profiling of individual cells using nanoliter droplets. Cell 2015;161:1202–14.

Mezentsev A, Nikolaev A, Bruskin S. Matrix metalloproteinases and their role in psoriasis. Gene 2014;540:1–10.

Milakovic M, Gooderham MJ. Phosphodiesterase-4 inhibition in psoriasis. Psoriasis (Auckl) 2021;11:21–9.

Mrowietz U, Bachelez H, Burden AD, Rissler M, Sieder C, Orsenigo R, et al. Secukinumab for moderate-to-severe palmoplantar pustular psoriasis: results of the 2PRECISE study. J Am Acad Dermatol 2019;80:1344–52.

Nedoszytko B, Sokołowska-Wojdyło M, Ruckemann-Dziurdzińska K, Roszkiewicz J, Nowicki RJ. Chemokines and cytokines network in the pathogenesis of the inflammatory skin diseases: atopic dermatitis, psoriasis and skin mastocytosis. Postepy Dermatol Alergol 2014;31:84–91.

Parisi R, Iskandar IYK, Kontopantelis E, Augustin M, Griffiths CEM, Ashcroft DM, et al. National, regional, and worldwide epidemiology of psoriasis: systematic analysis and modelling study. BMJ 2020;369:m1590.

Peixoto C, Joncour A, Temal-Laib T, Tirera A, Dos Santos A, Jary H, et al. Discovery of clinical candidate GLPG3970: a potent and selective dual SIK2/SIK3 inhibitor for the treatment of autoimmune and inflammatory diseases. J Med Chem 2024;67:5233–58.

Reynolds G, Vegh P, Fletcher J, Poyner EFM, Stephenson E, Goh I, et al. Developmental cell programs are co-opted in inflammatory skin disease. Science 2021;371:eaba6500.

Säll J, Pettersson AM, Björk C, Henriksson E, Wasserstrom S, Linder W, et al. Salt-inducible kinase 2 and -3 are downregulated in adipose tissue from obese or insulin-resistant individuals: implications for insulin signalling and glucose uptake in human adipocytes. Diabetologia 2017;60:314–23.

Sbidian E, Chaimani A, Garcia-Doval I, Doney L, Dressler C, Hua C, et al. Systemic pharmacological treatments for chronic plaque psoriasis: a network meta-analysis. Cochrane Database Syst Rev 2022;5:CD011535.

Schäbitz A, Hillig C, Mubarak M, Jargosch M, Farnoud A, Scala E, et al. Spatial transcriptomics landscape of lesions from non-communicable inflammatory skin diseases. Nat Commun 2022;13:7729.

Schafer PH, Parton A, Capone L, Cedzik D, Brady H, Evans JF, et al. Apremilast is a selective PDE4 inhibitor with regulatory effects on innate immunity. Cell Signal 2014;26:2016–29.

Schafer PH, Parton A, Gandhi AK, Capone L, Adams M, Wu L, et al. Apremilast, a cAMP phosphodiesterase-4 inhibitor, demonstrates anti-inflammatory activity in vitro and in a model of psoriasis. Br J Pharmacol 2010;159:842–55.

Schett G, Sloan VS, Stevens RM, Schafer P. Apremilast: a novel PDE4 inhibitor in the treatment of autoimmune and inflammatory diseases. Ther Adv Musculoskelet Dis 2010;2:271–8.

Shi F. Understanding the roles of salt-inducible kinases in cardiometabolic disease. Front Physiol 2024;15:1426244.

Sieminska I, Pieniawska M, Grzywa TM. The immunology of psoriasis-current concepts in pathogenesis. Clin Rev Allergy Immunol 2024;66:164–91.

Simpson-Abelson MR, Hernandez-Mir G, Childs EE, Cruz JA, Poholek AC, Chattopadhyay A, et al. CCAAT/enhancer-binding protein β promotes pathogenesis of EAE. Cytokine 2017;92:24–32.

Sun L, Liu W, Zhang LJ. The role of toll-like receptors in skin host defense, psoriasis, and atopic dermatitis. J Immunol Res 2019;2019:1824624.

Sung PS, Chang WC, Hsieh SL. CLEC5A: a promiscuous pattern recognition receptor to microbes and beyond. Adv Exp Med Biol 2020;1204:57–73.

Terui T, Kobayashi S, Okubo Y, Murakami M, Zheng R, Morishima H, et al. Efficacy and safety of guselkumab in Japanese patients with palmoplantar pustulosis: a phase 3 randomized clinical trial. JAMA Dermatol 2019;155:1153–61.

Terui T, Okubo Y, Kobayashi S, Sano S, Morita A, Imafuku S, et al. Efficacy and safety of apremilast for the treatment of Japanese patients with palmoplantar pustulosis: results from a Phase 2, randomized, placebo-controlled study. Am J Clin Dermatol 2023;24:837–47.

Van Muijen ME, Thomas SE, Groenewoud HMM, Otero ME, Ossenkoppele PM, Njoo MD, et al. Direct comparison of real-world effectiveness of biologics for psoriasis using absolute and relative psoriasis area and severity index scores in a prospective multicentre cohort. Acta Derm Venereol 2022;102:adv00712.

Wolf FA, Angerer P, Theis FJ. SCANPY: large-scale single-cell gene expression data analysis. Genome Biol 2018;19:15.

Wolock SL, Lopez R, Klein AM. Scrublet: Computational identification of cell doublets in single-cell transcriptomic data. Cell Syst 2019;8:281–91.e9.

Wu D, Hailer AA, Wang S, Yuan M, Chan J, El Kurdi A, et al. A single-cell atlas of IL-23 inhibition in cutaneous psoriasis distinguishes clinical response. Sci Immunol 2024;9:eadi2848.

Xu C, Lopez R, Mehlman E, Regier J, Jordan MI, Yosef N. Probabilistic harmonization and annotation of single-cell transcriptomics data with deep generative models. Mol Syst Biol 2021;17:e9620.

Zheng C, Li J, Chen H, Ma X, Si T, Zhu W. Dual role of CD177 + neutrophils in inflammatory bowel disease: a review. J Transl Med 2024;22:813.

Zhou C, Gao Y, Ding P, Wu T, Ji G. The role of CXCL family members in different diseases. Cell Death Discov 2023;9:212.

This work is licensed under a Creative Commons Attribution 4.0 International License. To view a copy of this license, visit http://creativecommons.org/licenses/by/4.0/

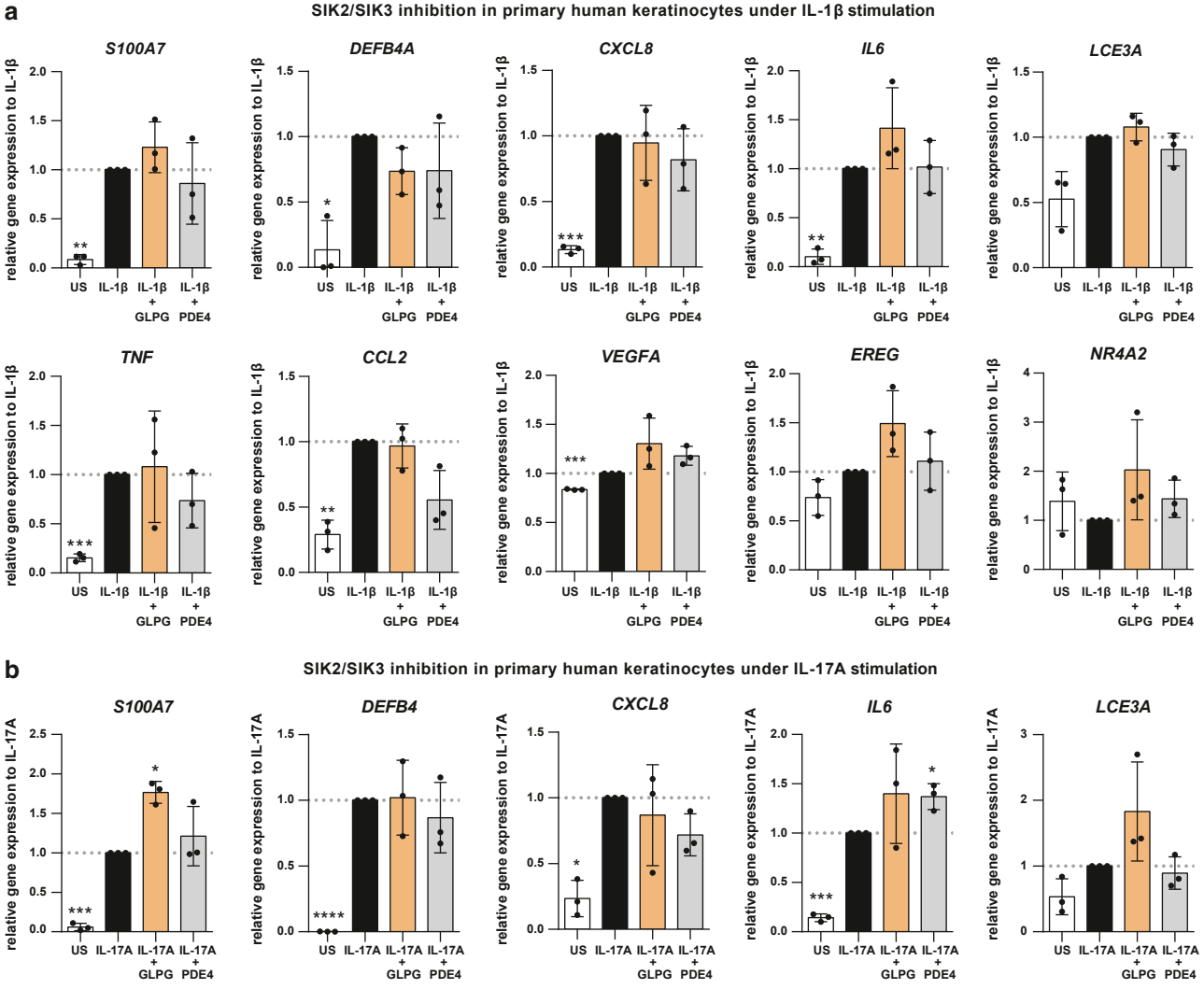
SUPPLEMENTARY MATERIALS AND METHODS

Keratinocytes

Keratinocytes were isolated from healthy donors by suction blisters and cultivated as previously described (Garzorz-Stark et al, 2018) in DermaLife Basal Medium supplemented with DermaLife K LifeFactor Kit (Lifeline Cell Technology, LL-0007) at 37 °C, 5% carbon dioxide. Second- to third-passage keratinocytes were grown to 60−80% confluence; starved for 5 hours in DermaLife Basal Medium; and pre-incubated for 1 hour with 10 μM GLPG3970, 2 μM apremilast, or vehicle (0.1% DMSO). Cells were stimulated with 50 ng/ml recombinant human IL-17A (R&D Systems, 317-ILB-050) or 50 ng/ml recombinant human IL-1β (PromoCell, C-61120) for 16 hours in the presence of the test compounds. Hydrocortisone was omitted from the medium for stimulation. Gene expression was analyzed by real-time qPCR.

SUPPLEMENTARY REFERENCE

Garzorz-Stark N, Lauffer F, Krause L, Thomas J, Atenhan A, Franz R, et al. Toll-like receptor 7/8 agonists stimulate plasmacytoid dendritic cells to initiate TH17-deviated acute contact dermatitis in human subjects. J Allergy Clin Immunol 2018;141:1320−33.e11.



Supplementary Figure S1. In vitro inhibition of SIK2 and SIK3 by GLPG3970 treatment in primary human keratinocytes. Primary human keratinocytes were preincubated with 10 μM GLPG3970 (GLPG), 2 μM apremilast (PDE4), or vehicle (0.1% DMSO) for 1 hour and stimulated with 50 ng/ml of (**a**) IL-1β or (**b**) IL-17A overnight. RNA was extracted and analyzed by real-time qPCR. Comparison of treatment group to reference group IL-1β or IL-17A was performed using Welch's t-test. $*P \leq .05$, $**P \leq .01$, and $***P \leq .001$. GLPG denotes GLPG3970 (SIK2/SIK3 inhibitor). US denotes unstimulated. PDE4, phosphodiesterase 4; SIK, salt-inducible kinase..

Supplementary Table S1. IC_{50} Values of GLPG3970 and Apremilast for Distinct Cytokines in Different Cell Types

Compound	hMO (LPS) TNF	hMO (LPS) IL-12	hMdM (LPS) TNF	hPBMC (αCD3/αCD28) IL-2
GLPG3970				
IC_{50} (nM)	118	103	240	770
n (donors)	8	8	4	4
Apremilast				
IC_{50} (nM)	33	27	103	69
n (donors)	8	8	4	4

Abbreviations: IC_{50}, half-maximal inhibitory concentration; LPS, lipopolysaccharide; hMdM, human monocyte-derived macrophage; hMO, human monocyte; hPBMC, human PBMC.
hMOs, hMdMs, and hPBMCs were stimulated with LPS or αCD3/αCD28 for 24 hours each. TNF, IL-12, and IL-2 were quantified using custom-developed ELISA protocols optimized for sensitivity and specificity (capture and detection antibodies were from R&D Systems and BD Pharmingen).

Supplementary Table S2. Primer Sequences of the fw and rev Primers Used in the Real-Time qPCR

Gene	Species		Sequence (5′−3′)
18S	Human	fw	GTAACCCGTTGAACCCCATT
		rev	CCATCCAATCGGTAGTAGCG
CCL2	Human	fw	TCCCAAAGAAGCTGTGATCTTCA
		rev	TTTGCTTGTCCAGGTGGTCC
CXCL5	Human	fw	CAGACCACGCAAGGAGTTCA
		rev	TCTTCAGGGAGGCTACCACT
CXCL8	Human	fw	ACCGGAAGGAACCATCTCAC
		rev	GGCAAAACTGCACCTTCACAC
DEFB4A	Human	fw	AAGGTGGAAGGCTTGATGTCC
		rev	TACCACCAAAAACACCTGGAA
EREG	Human	fw	CTGCCTGGGTTTCCATCTTCT
		rev	TTGAGCCACACGTGGATTGT
IL6	Human	fw	TTCGGTCCAGTTGCCTTCTC
		rev	TACATGTCTCCTTTCTCAGGGC
LCE3A	Human	fw	GAGTCACCACAGATGCC
		rev	CTTGCTGACCACTTCCC
NR4A2	Human	fw	AAACAAAGGCACATTGGCGG
		rev	GCCTGTCCAATCTCCTCCTTAG
S100A7	Human	fw	TCCAAACACACACATCTCACT
		rev	TCTTGTCATCACGTCTGGTGT
TNF	Human	fw	TGTTGTAGCAAACCCTCAAGC
		rev	ATGAGGTACAGGCCCTCTGA
VEGFA	Human	fw	AGCTGCGCTGATAGACATCC
		rev	CTACCTCCACCATGCCAAGT

Abbreviations: fw, forward; rev, reverse.